The Numerical Assessment of Cerebral Blood Flow in Immature Brain of Preterm Infants * **

Irina Sidorenko[1][0000−0003−4158−9416], Varvara Turova[2][0000−0002−6613−3311], Andrey Kovtanyuk[2][0000−0002−3286−110X], and Renée Lampe[2][0000−0002−1016−0249]

[1] Mathematical Faculty, Chair of Mathematical Modelling, Technical University of Munich, Garching, Germany sidorenk@ma.tum.de

[2] School of Medicine, Klinikum rechts der Isar, Orthopedic Department, Research Unit for Pediatric Neuroorthopedics and Cerebral Palsy of the Buhl-Strohmaier Foundation, Technical University of Munich, Munich, Germany turova@ma.tum.de, andrei.kovtaniuk@tum.de, renee.lampe@tum.de

Abstract. Intracerebral hemorrhage is the most dangerous complication in the development of premature infants. It is strongly connected with disturbances in cerebral blood flow (CBF) and fragility of small blood vessels in germinal matrix (GM), which is a highly vascularized layer of the premature brain. Permanent control of CBF value and its reaction on changes in mean arterial pressure (MAP), arterial carbon dioxide partial pressure (pCO_2), and oxygen partial pressure (pO_2) are of great importance in the clinical treatment of preterm newborns. The mathematical model for the calculation of CBF in immature brain, earlier proposed by Nikolai Botkin and his colleagues, included the dependence of the number of cerebral vessels, their diameter and length on the gestational age, volume of GM and brain weight. Furthermore, the vascular response of CBF to the change of MAP and pCO_2 was incorporated into the model by increasing or decreasing the diameter of blood vessels (i.e. vasodilation or vasoconstriction). The objective of the present study is modeling of pO_2 effect on CBF in the immature brain of preterm infants by accounting the phenomenological (experimental) dependence of CBF on pO_2 changes. Numerically calculated CBF reactivity to changes of MAP, pCO_2 and pO_2 demonstrates similar values as those observed in experimental studies. The developed mathematical model for CBF calculation can be a useful tool in both theoretical research of blood circulation and clinical nursing of preterm infants.

Keywords: Cerebral blood flow · Preterm infant · Immature brain · Germinal matrix · Intracerebral hemorrhage · Mean arterial pressure · Carbon dioxide partial pressure · Oxygen partial pressure.

1   Introduction

According to the World Health Organization statistics, more than 10% of infants are born preterm, i.e. before 37 completed weeks of gestation, and the preterm birth rate is increasing worldwide [3]. Intracranial hemorrhage (ICH) is the major complication of the preterm birth that occurs in 20% to 25% of neonates born before the 30th week of gestation (WG) and/or with body weight less than 1500 grams at birth [31]. It often leads to lifelong impairment, such as cerebral palsy, and may cause permanent disorder of the postural and musculoskeletal system, learning disabilities, behavioral problems, speech disorders, perception deficits and seizure disorders. ICH typically originates in the germinal matrix (GM) [1], which is a highly vascularized area of the developing brain. Volumetric analysis of the germinal matrix provided using 3D MR measurements [20] has shown that the GM reaches its maximum size at 23 WG and practically disappears by 34 WG. A highly fragile microvessel network of GM is vulnerable to destruction, which may occur due to the spontaneous fluctuations of cerebral blood flow (CBF) caused by the impaired autoregulation [35]. Due to this, the continuous monitoring of CBF is important issue in clinical nursing of preterm infants. During the last decades, several techniques, such as near-infrared spectroscopy [12], Xenon-133 clearance measurements [19], transcranial Doppler ultrasonography [27], MRI based arterial spin labeling [11], and diffusion correlation spectroscopy [12] became available for measurements of the entire brain CBF. However, none of these techniques are currently used in neonatal clinical practice for the regular monitoring of CBF. The numerical assessment of CBF using standard clinical records [4, 5, 21, 30] may become a promising approach for clinical applications.

The previous mathematical models [21, 29, 30] evaluated CBF from the brain weight (BW) estimated from the gestational age (GA), mean arterial pressure (MAP), and carbon dioxide partial pressure (pCO_2) available from the standard clinical records. The arterial oxygen partial pressure (pO_2) is another important clinically measured parameter that affects CBF. There is evidence [22, 25] that the brain reacts to pO_2 changes by inverse CBF changes, which is described by negative pO_2 reactivity. Moderate changes in arterial pO_2 do not influence CBF noticeably. Acute hypoxia causes an increase in CBF via vasodilation of cerebral arteries and arterioles [14, 26]. This elevation appears to be a threshold phenomenon [22]: CBF does not change until pO_2 falls below 50 mmHg [10, 18], but beneath this limit CBF increases substantially [22, 24]. A strong decrease of pO_2 can increase CBF up to 400%, comparing to normoxia condition [7, 18].

While CBF is greatly increased by a reduction in pO_2, the elevation of pO_2 level typically causes less pronounced, but regular reduction in CBF [34]. The study [26] has shown significant decrease in CBF velocity in 15 of the 17 premature infants with hyperoxia during the first few days of life.

The purpose of the present work is accounting for the effect of pO_2 on CBF in the immature brain of preterm infants. The enhancement of the mathematical model for CBF calculation [21, 30] is performed by altering the vessels' diameter during hypoxia or hyperoxia as a response to changes in arterial pO_2 [14, 26].

2   Methods

2.1   Modeling of CBF in the Immature Brain with a Germinal Matrix

A mathematical model for the calculation of CBF [21, 30] is based on a hierarchical cerebrovascular model for the adult brain [29] in which the cerebral vascular system is described by 19 levels according to the morphological characteristics of the vessels. Levels from 1 to 9 correspond to arteries and arterioles, level 10 accounts for capillaries, and levels from 11 to 19 simulate venules and veins. To adjust the model to the immature brain, the number of vessels m_j as well as their length l_j and diameter d_j are scaled down on each level j according to the brain weight (BW) of infant as follows:

$$m_j = M_j \cdot \left(1200/BW - (1200/BW - 1) \cdot |j - 10|/9\right)^{-1}, \tag{1}$$

$$l_j = L_j \cdot \left(1 + 0.1 \cdot (1200/BW - 1) \cdot |j - 10|/9\right)^{-1}, \tag{2}$$

$$d_j = D_j \cdot \left(1 + 0.1 \cdot (1200/BW - 1) \cdot |j - 10|/9\right)^{-1}. \tag{3}$$

Here, M_j, L_j and D_j are the number, the length, and the diameter of vessels in level j of the adult brain, respectively, and the value of 1200 g corresponds to the approximate weight of the adult brain [29]. The coefficient 0.1 is used to scale the vessel length and diameter to the experimental measurements [2, 32]. The brain weight of the preterm infant (BW) is computed from the gestational age in weeks (WG) according to the regression formula [16]:

$$BW(WG) = 255.25 - 35.44 \cdot WG + 1.52 \cdot WG^2 - 0.01 \cdot WG^3. \tag{4}$$

Such a model keeps the number of main arteries and veins constant across age and increases the number of arterioles, capillaries and venules according to the amount of the brain tissue, which grows with age. In contrast to the vessel's number, the length and diameter rise with age for large vessels, but remain the same for capillaries.

Anatomic analysis of blood vessels in a germinal matrix [1, 2, 32] have shown, that their morphological and histological characteristics are close to other brain capillaries. Therefore, the presence of GM is modeled as an additional parallel circuit on the capillary level $(j = 10)$. The number of non-GM capillaries in the larger circuit is given by:

$$m_B = M_{10}/(1200/BW) \cdot (1 - GM_{vf}). \tag{5}$$

The number of GM capillaries in the smaller circuit is given by:

$$m_{GM} = M_{10}/(1200/BW) \cdot GM_{vf} \cdot 1.5. \tag{6}$$

Here, M_{10} is the number of capillaries on the 10th level of the adult vascular network [29], GM_{vf} is the volume fraction of the germinal matrix relative to the

total brain volume [20], and the factor 1.5 describes a vascular density correction factor [2] for the GM. The values of capillary length and diameter are taken from the literature as follows: $l_{GM} = 40$ μm, $d_{GM} = 6.7$ μm for the GM [2, 32], and $l_B = 60$ μm and $d_B = 5.6$ μm for the rest of the brain [29].

The total CBF is calculated from the Kirchhoff's law as follows:

$$CBF = (MAP - P_{ic}) \cdot \left(\sum_{j=1}^{19} RES_j^{level} \right)^{-1}. \tag{7}$$

Here, P_{ic} is the intracranial pressure taken for preterm infants as 5 mmHg [13] and RES_j^{level} is the total vascular resistance of the level j. All levels except for the capillary one consist of m_j parallel connected vessels with the individual resistance RES_j. Thus, the total resistance can be calculated as follows:

$$RES_j^{level} = RES_j/m_j. \tag{8}$$

The total resistance of the capillary level $j = 10$, consisting of two parallel circuits (GM and non-GM capillaries), can be calculated as:

$$RES_{10}^{level} = \left((RES_{GM}/m_{GM})^{-1} + (RES_B/m_B)^{-1} \right)^{-1}. \tag{9}$$

The resistances RES_j, RES_B, and RES_{GM} are calculated using a micropolar fluid model [15, 28]. Thus, the conservation of angular momentum results in new equations describing the rotation of fluid particles on the micro-scale [17, 33].

2.2 Accounting for Arterial pO_2

According to the experimental data, the effect of the pO_2 on CBF is different for three different states: hypoxia with $pO_2 < 50$ mmHg, normoxia with 50 mmHg $\leq pO_2 \leq 70$ mmHg, and hyperoxia with $pO_2 > 70$ mmHg. Experimental study [25] has shown that the direct effect of pO_2 on CBF in normoxia state was about 10 times less than the effect of pCO_2, suggesting that the influence of pO_2 on CBF in this case is negligible. Therefore, in the mathematical model presented here, the effect of pO_2 in normoxia is neglected. The effect of pO_2 in hyperoxia or hypoxia is modeled by the decrease or increase of the vessels' diameter. An important point is that pO_2 and pCO_2 influence blood circulation independently of each other and have an additive effect on the vessel diameter [14, 26]. In the mathematical model, first the influence of pCO_2 on the reference diameter of the vessel is accounted for, as described in [30], and then the effect of pO_2 is added. The myogenic response to the MAP changes is included afterwards as it is specified in [30].

The vasodilation during hypoxia and vasoconstriction during hyperoxia is calculated as a linear increase or decrease of the vessel diameter as:

$$d_{pO_2} = d_{pCO_2} + pv * d_{pCO_2}. \tag{10}$$

Here, d_{pCO_2} is the diameter of the vessel after accounting for the pCO_2 effect as described in [30]. The coefficient pv depends on vessel type and is equal to the relative change of the vessel's diameter measured in animal experiments [14, 26]. Neither dilations nor constrictions due to pO_2 alterations were detected for capillaries. During hypoxia, a more obvious vasodilation in the veins than in the arteries was observed. In mild hypoxia, with 40 mmHg $\leq pO_2 < 50$ mmHg, an increase from the reference diameter size was 6% for arteries and 9% for veins. Furthermore, in severe hypoxia, with $pO_2 < 40$ mmHg, the diameter increased by 20% for arteries and by 34% for veins. While hypoxia caused considerable increases in blood flow, hyperoxia produced only a moderate decrease. During hyperoxia, both arteries and veins constricted slightly and similarly. In mild hyperoxia, with 70 mmHg $< pO_2 \leq 80$ mmHg, a decrease from the reference diameter size was 5% for arteries and 6% for veins, while in severe hyperoxia, with $pO_2 > 80$ mmHg, the decrease was 7% both for arteries and for veins.

3   Results and Discussion

The number of vessels on different levels of the hierarchical cerebrovascular model versus gestational age in weeks is shown in Fig. 1. While the number of large arteries ($j = 1$) and veins ($j = 19$) stays constant, the number of smaller vessels ($2 \leq j \leq 18$) increases with gestational age. On capillary level ($j = 10$), the number of non-GM capillaries also grows with gestational age, whilst the number of GM capillaries rapidly decreases and becomes zero after 33 WG (see Fig. 1b). This is in agreement with the observation that the number of ICH cases rapidly decreases after 34 WG [1].
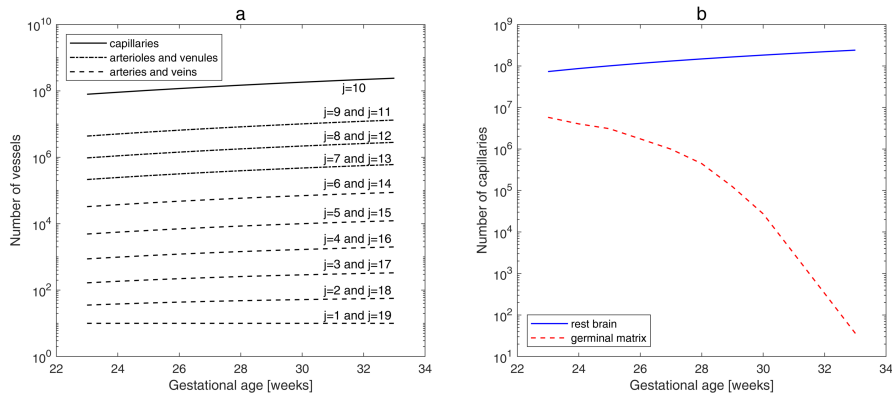
Fig. 1. Number of vessels for different gestational ages on different levels of the hierarchical cerebral vascular model (a) and on the capillary level (b).

The initial vessel diameter slowly increases with gestational age (see Fig. 2a). The CBF reactivity on changes in pO_2, pCO_2, and MAP is regulated by the vascular activity, i.e. vasoconstriction and vasodilation, which is modeled as the alteration of the vessel's diameter. The effect of pO_2 changes on diameters of the largest arteries and veins is demonstrated in Fig. 2b. The most considerable alteration of the vessel's diameter is observed for veins during hypoxia. The diameter of the largest veins increases from 1.53 mm to 2.1 mm at age 23 WG and from 2.37 mm to 3.2 mm at age 33 WG.
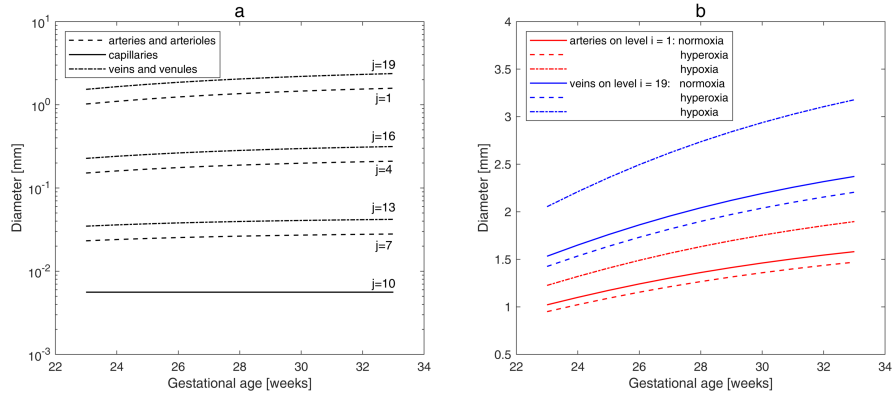
Fig. 2. Initial diameter of vessels for different gestational ages on different levels of the hierarchical cerebral vascular model (a) and at different values of pO_2 (b).

The dependence of CBF on changes in pO_2, pCO_2, and MAP is demonstrated in Fig. 3. The CBF stays constant for pO_2 values between 50 mmHg and 70 mmHg, as it have been described in [10, 18]. In hypoxia condition, CBF demonstrates a considerable increase with a threshold phenomenon at $pO_2 = 50$ mmHg described in [18, 22]. At $pO_2 = 50$ mmHg, CBF starts to increase with decreasing pO_2, reaching a twofold elevation of CBF value with respect to normoxia level (see Fig. 3a) at $pO_2 = 30$ mmHg, as it has been observed in [8, 18]. In hyperoxia condition, the increase of pO_2 from 70 mmHg to 80 mmHg causes the 20% decrease in CBF (see Fig. 3a). Such a reactivity is in good agreement with experimental studies [6, 8, 23], where CBF reactivity of $10-30\%$ per 1 kPa (7.5 mmHg) increase of arterial pO_2 was measured in preterm infants.

Simultaneous dependence of CBF on MAP, pCO_2, and pO_2 is shown on Figure 3b. Whilst the CBF reactivity on pCO_2 changes has linear behavior, the CBF reactivity on MAP demonstrates a plateau which corresponds to the cerebral autoregulation observed in experiments [1, 9]. The calculated values of CBF and its reactivity to changes in main medical parameters are in good agreement with experimental measurements presented in the literature [1, 6, 8–10, 18, 22, 23]. Thus, the mathematical model developed provides a realistic description

of physiological processes and can be proposed as a useful tool both for the theoretical research of cerebral circulation and the clinical nursing of preterm infants.
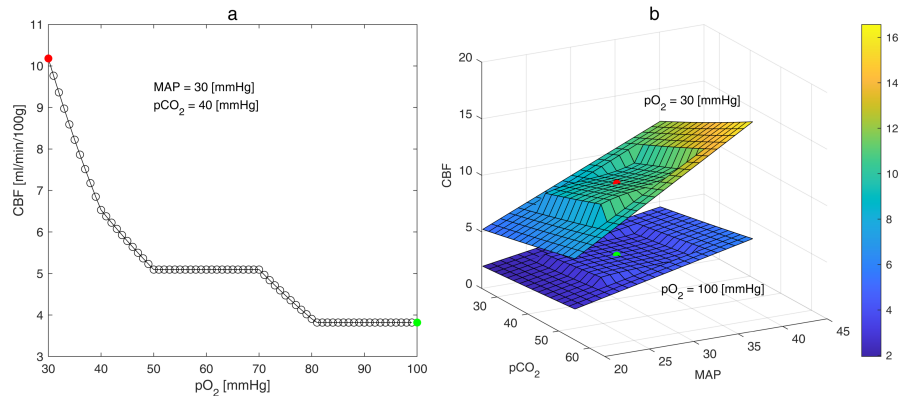
Fig. 3. Dependence of CBF on pO_2 (a), pCO_2 and MAP (b). Both plots correspond to the 23 WG. The red and green points in both plots correspond to the same values of pO_2, pCO_2 and MAP.

References

1. Ballabh, P.: Intraventricular hemorrhage in premature infants: mechanism of disease. Pediatr. Res. **67**(1), 1–8 (2010). https://doi.org/10.1203/PDR.0b013e3181c1b176

2. Ballabh, P., Braun, A., Nedergaard, M.: Anatomic analysis of blood vessels in germinal matrix, cerebral cortex, and white matter in developing infants. Pediatr. Res. **56**(1), 117–24 (2004). https://doi.org/10.1203/01.PDR.0000130472.30874.FF

3. Blencowe, H., Cousens, S., Chou, D., Oestergaard, M., Say, L., Moller, A.B., Kinney, M., Lawn, J.: Born too soon: the global epidemiology of 15 million preterm births. Reprod. Health. **10**, S2 (2013). https://doi.org/10.1186/1742-4755-10-S1-S2

4. Botkin, N., Turova, V., Lampe, R.: Feedback control of impaired cerebral autoregulation in preterm infant: Mathematical modelling. In: 25th Mediterranean Conference on Control and Automation (MED), pp. 229–234. IEEE, Valletta (2017). https://doi.org/10.1109/MED.2017.7984123

5. Botkin, N.D., Turova, V.L., Kovtanyuk, A.E., Sidorenko, I.N., Lampe R.: Extended model of impaired cerebral autoregulation in preterm infants: Heuristic feedback control. Math. Biosci. Eng. **16**(4), 2334–2352, (2019). https://doi.org/10.3934/mbe.2019117

6. Brew, N., Walker, D., Wong, F. Y.: Cerebral vascular regulation and brain injury in preterm infants. Am. J. Physiol. Reg., Integr. Compar. Physiol. **306**(11), R773–R786 (2014). https://doi.org/10.1152/ajpregu.00487.2013

7. Cipolla, M.J.: The cerebral circulation. Colloquium Series on Integrated Systems Physiology: From Molecule to Function, **1**(1), 1–59 (2009). https://doi.org/10.4199/C00005ED1V01Y200912ISP002

8. Cold, G.E., Dahl, B.L.: Topics in neuroanaesthesia and neurointensive care: Experimental and clinical studies upon cerebral circulation, metabolism and intracranial pressure. Springer, Berlin, Heidelberg (2002). https://doi.org/10.1007/978-3-662-04845-0

9. Da Costa, C.S., Czosnyka, M., Smielewski, P., Mitra, S., Stevenson, G.N., Austin, T.: Monitoring of cerebrovascular reactivity for determination of optimal bloodpressure in preterm infants. J. Pediatr. **167**(1), 86–91 (2015). https://doi.org/10.1016/j.jpeds.2015.03.041

10. Deorari, A.K.: Blood gas analysis. Deorari, AIIMS (2008)

11. De Vis, J.B., Hendrikse, J., Groenendaal, F., De Vries, L.S., Kersbergen, K.J., Benders, M.J., Petersen, E.T.: Impact of neonate haematocrit variability on the longitudinal relaxation time of blood: Implications for arterial spin labelling MRI. Neuroimage. Clin. **4**, 517–525 (2014). https://doi.org/10.1016/j.nicl.2014.03.006

12. Diop, M., Kishimoto, J., Toronov, V., Lee, D.S., Lawrence, K.S.: Development of a combined broadband near-infrared and diffusion correlation system for monitoring cerebral blood flow and oxidative metabolism in preterm infants. Biomed. Opt. Express. **6**(10), 3907–18 (2015). https://doi.org/10.1364/BOE.6.003907

13. Easa, D., Tran, A., Bingham, W.: Noninvasive intracranial pressure measurement in the newborn: an alternate method. Am. J. Dis. Child. **137**(4), 332–335 (1983). https://doi.org/10.1001/archpedi.1983.02140300014004

14. Eperon, G., Johnson, M., David, N.J.: The effect of arterial PO2 on relative retinal blood flow in monkeys. Investi. Ophthalmol. **14**(5), 342–352 (1975)

15. Erdogan, M.E.: Polar effects in the apparent viscosity of a suspension. Rheol. Acta. **9**(3), 434–438 (1970). https://doi.org/10.1007/BF01975413

16. Guihard-Costa, A.M., Larroche, J.C.: Differential growth between the fetal brain and its infratentorial part. Early Hum. Dev. **23**(1), 27–40 (1990). https://doi.org/10.1016/0378-3782(90)90126-4

17. Hoffmann, K.-H., Marx, D., Botkin, N.D.: Drag on spheres in micropolar fluids with non-zero boundary conditions for microrotations. J. Fluid Mech. **590**, 319–330 (2007). https://doi.org/10.1017/S0022112007008099

18. Johnston, A.J., Steiner, L.A., Gupta, A.K., Menon D.K.: Cerebral oxygen vasoreactivity and cerebral tissue oxygen reactivity. Br. J. Anaesth. **90**(6), 774–786 (2003). https://doi.org/10.1093/bja/aeg104

19. Jayasinhe, D., Gill, A.B., Levene, M.I.: CBF reactivity in hypotensive and normotensive preterm infants. Pediatr Res. **54**(6), 848–853 (2003). https://doi.org/10.1203/01.PDR.0000088071.30873.DA

20. Kinoshita, Y., Okudera, T., Tsuru, E., Yokota, A.: Volumetric analysis of the germinal matrix and lateral ventricles performed using MR images of postmortem fetuses. Am. J. Neuroradiol. **22**(2), 382–388 (2001)

21. Lampe, R., Botkin, N., Turova, V., Blumenstein, T., Alves-Pinto, A.: Mathematical modelling of cerebral blood circulation and cerebral autoregulation: towards preventing intracranial hemorrhages in preterm newborns. Comput. Math. Methods. Med. **2014**, 965275 (2014). https://doi.org/10.1155/2014/965275

22. Lassen, N., A.: Control of cerebral circulation in health and disease. Circ. Res. **34**(6), 749–760 (1974). https://doi.org/10.1161/01.RES.34.6.749

23. Leahy, F. A., Cates, D., MacCallum, M., Rigatto, H.: Effect of CO2 and 100% O2 on cere-bral blood flow in preterm infants. J. Appl. Physiol. **48**(3), 468–472 (1980). https://doi.org/10.1152/jappl.1980.48.3.468

24. Masamoto, K., Tanishita, K.: Oxygen transport in brain tissue. J. Biomech. Eng. **131**(7), 074002 (2009). https://doi.org/10.1115/1.3184694

25. Menke, J., Michel, E., Rabe, H., Bresser, B. W., Grohs, B., Schmitt, R. M., Jorch, G.: Simultaneous influence of blood pressure, PCO2, and PO2 on cerebral blood flow velocity in preterm infants of less than 33 weeks' gestation. Pediatr. Res. **34**(2), 173–177 (1993). https://doi.org/10.1203/00006450-199308000-00014

26. Niijima, S., Shortland, D.B., Levene, M.I., Evans, D.H.: Transient hyperoxia and cerebral blood flow velocity in infants born prematurely and at full term. Arch. Dis. Child. **63**(10 Spec No), 1126–1130 (1988). https://doi.org/10.1136/adc.63.10_spec_no.1126

27. Noori, S., Anderson, M., Soleymani, S., Seri, I.: Effect of carbon dioxide on cerebral blood flow velocity in preterm infants during postnatal transition. Acta Paediatr. **103**(8), e334–e339 (2014). https://doi.org/710.1111/apa.12646

28. Papautsky, I., Brazzle, J., Ameel, T., Frazierac, A.B.: Laminar fluid behavior in microchannels using micropolar fluid theory. Sens. Actuat. A. Phys. **73**(1-2), 101–108 (1999). https://doi.org/710.1016/S0924-4247(98)00261-10

29. Piechnik, S.K., Chiarelli, P.A., Jezzard, P.: Modelling vascular reactivity to investigate the basis of the relationship between cerebral blood volume and flow under CO2 manipulation. Neuroimage **39**(1), 107–118 (2008). https://doi.org/10.1016/j.neuroimage.2007.08.022

30. Sidorenko, I., Turova, V., Botkin, N., Eckardt, L., Alves-Pinto, A., Felderhoff-Müser, U., Rieger-Fackeldey, E., Kovtanyuk, A., Lampe, R.: Modeling cerebral blood flow dependence on carbon dioxide and mean arterial blood pressure in the immature brain with accounting for the germinal matrix. Front. Neurol. **9**, 812 (2018). https://doi.org/10.3389/fneur.2018.00812

31. Schmid, M.B., Reister, F., Mayer, B., Hopfner, R.J., Fuchs, H., Hummler, H.D.:Schmid, M.B., Reister, F., Mayer, B., Hopfner, R.J., Fuchs, H., Hummler, H.D.: Prospective risk factor monitoring reduces intracranial hemorrhage rates in preterm infants. Dtsch. Arztebl. Int. **110**(29-30), 489–496 (2013). https://doi.org/10.3238/arztebl.2013.0489
Prospective risk factor monitoring reduces intracranial hemorrhage rates in preterm infants. Dtsch. Arztebl. Int. **110**(29-30), 489–496 (2013). https://doi.org/10.3238/arztebl.2013.0489

32. Trommer, B.L., Groothuis, D.R., Pasternak, J.F.: Quantitative analysis of cerebral vessels in the newborn puppy: the structure of germinal matrix vessels may predispose to hemorrhage. Pediatr. Res. **22**(1), 23–28 (1987). https://doi.org/10.1203/00006450-198707000-00007

33. Turova, V., Botkin, N., Alves-Pinto, A., Blumenstein, T., Rieger-Fackeldey, E., Lampe, R.: Modelling autoregulation of cerebral blood flow using viability approach. In: International Symposium on Dynamic Games and Applications. **15**, 345–363. Birkhäuser, Cham (2016). https://doi.org/10.1007/978-3-319-70619-1_16

34. Ursino, M., Di Giammarco, P., Belardinelli, E.: A mathematical model of cerebral blood flow chemical regulation. I. Diffusion processes. IEEE Trans. Biomed. Eng. **36**(2), 183–191 (1989). https://doi.org/10.1109/10.16465

35. Wong, F.Y., Leung, T.S., Austin, T., Wilkinson, M., Meek, J.H., Wyatt, J.S., Walker, A.M.: Impaired autoregulation in preterm infants identified by using spatially resolved spectroscopy. Pediatrics **121**(3), e604–e611 (2008). https://doi.org/10.1542/peds.2007-1487